Design and Digital Twin of INFN's main Nb_3Sn 15T Dipole for CERN's FCC

TUE-PO1-110-03

C. Kokkinos[1], S. Farinon[2], T. Gortsas[3], S. Kokkinos[1], K. Loukas[1], A. Pampaloni[2], D. Polyzos[3], D. Rodopoulos[3]

1. FEAC Engineering P.C., Afstralias Str. 61, 26442, Patras, Greece, feacomp.com, info@feacomp.com
2. INFN (Istituto Nazionale di Fisica Nucleare Sezione di Genova), 16146 Genova, Italy
3. University of Patras, 26504 Rio Achaia, Greece

MT27 Nov. 15-19, 2021 Fukuoka, Japan

Abstract

CERN is currently investigating the feasibility of a future collider - the Future Circular Collider (FCC) - as a potential successor of the Large Hardon Collider (LHC), providing scientists in the field of high energy physics with a powerful discovery tool. INFN developed the main 16T Nb3Sn dipole of the FCC based on the cos-theta coil design. The baseline design of the superconducting magnet adopts the bladder-and-key concept and includes 4-layered asymmetric coils, an aluminum shell and a welded stain-less-steel skin. The scope of this collaborative work between INFN, CERN, UPATRAS & FEAC, is to validate and further study the baseline design.

Mechanical Structure

The main features of the 16T dipole design are illustrated in *Fig. 1*.

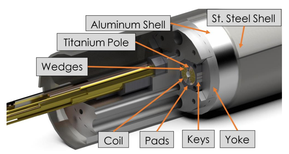

Fig. 1. Exploded view of the 16T Nb3Sn Dipole showing its key features.

- The Nb3Sn coil is asymmetric with respect to the vertical axis and it is based on the cos-theta design.
- The coils are epoxy impregnated with four winding layers.
- The copper wedges and ground insulation are epoxy-impregnated with the coil while the Ti-alloy coil pole blocks are not glued to the coil (pole-loading concept).

Mechanical Structure (cont.)

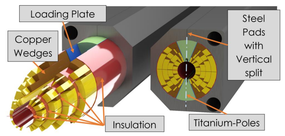

Fig. 2. FCC's main dipole coil cross section and key features, based on the pole loading concept. The coil is asymmetric with respect to the vertical axis.

- The Ø660 mm iron yoke is made in three pieces, with the central part acting as an iron barrier between the two apertures.
- The one-piece aluminum shell is 50-mm-thick while the 20-mm-thick st. steel outer shell is made in two halves and welded at the horizontal plane.
- The external diameter of the cold mass structure is 800 mm.

The shimming locations are presented in *Fig 3*.

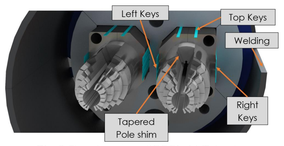

Fig. 3 Shim location of FCC's 16 T dipole.

- By adjusting the thickness of the keys, one can compensate the dimensional distortions (up to several tenths of mm) of the coils and the rest key components.
- The vertical keys between the pads and the yoke can compensate the tendency of the coil to become oval along the horizontal axis during powering.
- The top keys are used to ensure contact at the coil-pads interface in the pole region during powering.
- The welded shell encompasses the whole structure and the weld shrinkage provides pre-stress to the assembly at room temperature.
- During cooling down, the aluminum shell shrinks and provides further pre-stress as well.

EM Analysis

The 2D electromagnetic model is analysed in SIEMENS STAR-CCM+ [8], PITHIA [9], and ROXIE [10] to compare results between finite and boundary element method solvers. A non-linear B-H curve is used to describe the magnetization of the yoke. In PITHIA, only the boundaries of the model are meshed and internal points are added where the results are computed [11]. The electromagnetic forces computed in PITHIA (Table I) are mapped onto the structural mesh. The three different software calculated results with a maximum discrepancy of 2% compared to Table I. The 2D magnetic field distribution at 16.36 T is shown in *Fig. 4*.

TABLE I
MAGNETIC FORCES CALCULATED IN PITHIA

I [kA] (11.39)	B [T] (16.36)	Left Coil		Right Coil	
		Fx Sum [MN]	Fy Sum [MN]	Fx Sum [MN]	Fy Sum [MN]
Layer 1		-2.11	-0.142	2.09	-0.14
Layer 2		-2.38	-0.538	2.25	-0.47
Layer 3		-2.08	-1.15	2.0	-1.08
Layer 4		-0.54	-2.165	0.39	-2.0
SUM		-7.11	-3.995	6.73	-3.69

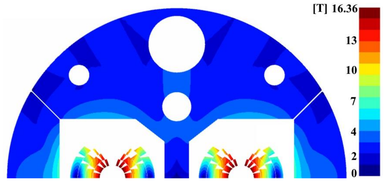

Fig. 4 Magnetic analysis of the magnet at 11.39 kA, 16.36 T in PITHIA.

Structural Analysis

A thermal-structural analysis of the baseline design is implemented to determine the structural integrity of the magnet. Four loading scenarios (LS) are considered in the FEM (*Fig 5.*)

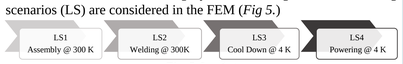

Fig. 5. Load steps

All shims are simulated by offsetting the contact and target faces by a distance equal to the shim thickness.

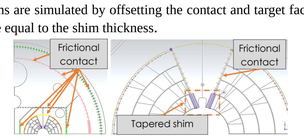

Fig. 6. Contacts and shim locations

The Von-Mises Stress (MPa) evolution for the four loading scenarios is shown in *Fig. 7 a*nd the maximum stress at the main components is presented in *Fig. 8*

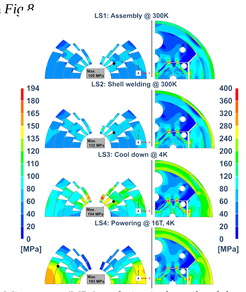

Fig. 7. Von-Mises stress (MPa) evolution in the coil and the whole structure

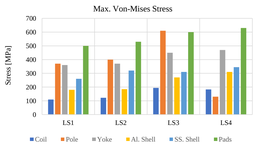

Fig. 8. Maximum stress at the main components of the structure

Sensitivity Analysis

The sensitivity analysis is conducted by utilizing the DoE method (Design of Experiments) which determines sampling points used to construct a response surface based on the Kriging method. Eight geometric and material input parameters (Table II) were chosen for this study.

TABLE II
PARAMETERS INCLUDED IN THE SENSITIVITY ANALYSIS

Parameter	Direction	Nominal Value	Tolerance
E_{coil}		27.5 GPa @ 300 K 30.25 GPa @ 4K	19 – 38 GPa 21 – 42 GPa
a_{coil}		3.2 mm/m	2.5 – 4 mm/m
Weld Shrinkage (per half shell)	Vertical	0.2 mm	-
Left Keys	Horizontal	0.0 mm	0 – 0.5 mm
Top Keys	Vertical	0.2 mm	0 – 0.8 mm
Right Keys	Horizontal	1.2 mm	0.6 – 1.8 mm
Tapered Pole Shim	Azimuthal	0.025 mm	0.01 – 0.04 mm
$t_{shell,aluminum}$		50 mm	20 – 60 mm
$t_{shell,st.steel}$		20 mm	10 – 30 mm

Table III presents the effect of the design parameters on the von-Mises stress of the coil at all load-steps, according to the tolerances described in Table II.

TABLE III
SENSITIVITY ANALYSIS RESULTS

Parameter	Coil von-Mises @ LS1 (nominal: 109 MPa)		Coil von-Mises @ LS2 (nominal: 122 MPa)	
	Range (MPa)	$\Delta\sigma_{max}$ (MPa)	Range (MPa)	$\Delta\sigma_{max}$ (MPa)
E_{coil}	123-107	16	136-118	18
a_{coil}	109-109	0	122-122	0
Left Keys	119-197	78	131-206	75
Top Keys	118-224	106	131-226	95
Right Keys	72-147	75	78-160	82
Tapered Pole Shim	109-110	1	121-123	2
$t_{shell,aluminum}$	87-118	31	96-130	34
$t_{shell,st.steel}$	91-125	34	98-142	44
	Coil von-Mises @ LS3 (nominal: 194 MPa)		Coil von-Mises @ LS4 (nominal: 183MPa)	
	Range (MPa)	$\Delta\sigma_{max}$ (MPa)	Range (MPa)	$\Delta\sigma_{max}$ (MPa)
E_{coil}	214-199	15	215-174	41
a_{coil}	191-225	34	170-215	45
Left Keys	205-249	44	194-230	36
Top Keys	205-252	47	177-346	169
Right Keys	120-238	118	198-216	18
Tapered Pole Shim	193-195	2	183-184	1
$t_{shell,aluminum}$	145-207	62	192-194	2
$t_{shell,st.steel}$	175-211	36	165-199	34

Optimized Design

The sensitivity analysis on the baseline design provided a better understanding on the behaviour of the structure, thus allowing for further optimization and fine-tuning of the design. The optimized set of assembly parameters is presented in Table IV.

TABLE IV
ASSEMBLY PARAMETERS OF BASELINE & OPTIMIZED DESIGN

Parameter	Nominal Value (baseline design)	Optimized design
Ø of Cold Mass structure	800 mm	780 mm
Weld Shrinkage (per half shell)	0.2 mm	0.15 mm
Left Keys	0.0 mm	0.0 mm
Top Keys	0.2 mm	0.25 mm
Right Keys	1.2 mm	1 mm
Tapered Pole Shim	0.025 mm	0.05 mm
$t_{shell,aluminum}$	50 mm	25 mm
$t_{shell,st.steel}$	20 mm	35 mm

The Von-Mises Stress (MPa) evolution for the four loading scenarios of the optimized design is shown in *Fig. 9* and the maximum stress at the main components is presented in *Fig 10*.

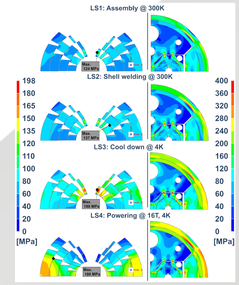

Fig. 9. Optimized design. Von-Mises stress (MPa) evolution in the coil and the whole structure

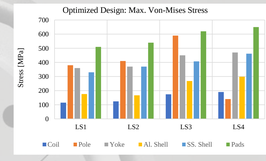

Fig. 10. Optimized design. Maximum stress at the main components of the structure

Conclusions

- The results from the electro-magnetic and the structural analysis have been cross-checked and verified by different users with the use of different software (Star-CCM+ vs. PITH-IA vs. ROXIE / Simcenter 3D vs. ANSYS), different numerical methodologies (FEM vs. BEM) and different solvers.
- The design showcases that coil pre-stress can be applied in a well-controlled manner and that the structure allows keeping the stress in the coil and the support structure within acceptable levels up to 16 T.
- The latest modifications in the baseline design of the 16 T main dipole and the computed results confirm the magnet support structure and its ability to manage the large level of Lorentz forces.
- The sensitivity analysis shows that the range of the various parameters used in the study cover a large design space. This is reflected at the range of the resulting maximum equivalent stress in the coil.
- At the magnet's nominal operation field of 16 T, the equivalent stress in the coil re-mains below 200 MPa for a big fraction of the parameter variations, which is a sign that there is margin in the design.
- The latest modifications in the baseline design of the 16 T main dipole and the computed results confirm the magnet support structure and its ability to manage the large level of Lorentz forces.
- To reduce the manufacturing cost of the magnet, an alter-native set of assembly parameters is presented, with reduced aluminum shell thickness. The structure proves that it can still operate within the safe limits by respecting the design goals.

References

[1] D. Schoerling et al., "The 16 T dipole development program for FCC and HE-LHC", IEEE Transactions on Applied Superconductivity, Vol. 29, No.5, Art. No. 4003109, September 2019.
[2] M. Benedikt *et al.*, Future Circular Collider Study. Volume 3: The Had-ron Collider (FCC-hh) Conceptual Design Report, CERN Accelerator Reports, CERN-ACC-2018-0058, Geneva, Switzerland, Dec. 2018.
[3] C. Kokkinos et al., "FEA Model and Mechanical Analysis of the Nb3Sn 15-T Dipole Demonstrator", IEEE Transactions on Applied Supercon-ductivity, Vol. 28, Issue 3, Art. No. 4007406, April 2018.
[4] Future Circular Collider Conceptual Design Report, https://fcc-cdr.web.cern.ch/.
[5] R. Valente *et al.*, "Baseline design of a 16T cos θ bending dipole for the future circular collider," IEEE Transactions on Applied Superconductiv-ity, vol. 29, no. 5, Art. No. 4003005, Aug. 2019.
[6] S. Caspi *et al.*, "The use of pressurized bladders for stress control of su-perconducting magnets," IEEE Transactions on Applied Superconduc-tivity, vol. 11, no. 1, pp. 2272–2275, Mar. 2001.
[7] C. Kokkinos and M. Karppinen, "High Gradient Nb3Sn Quadrupole Demonstrator MKQXF Engineering Design", IEEE Transactions on Applied Superconductivity, Vol. 28, Issue 3, Art. No. 4006008, April 2018.
[8] SIEMENS Simcenter 3D website. [Online]. Available:, www.plm.automation.siemens.com
[9] PITHIA BEM software package website. [Online]. Available:, www.feacomp.com/pithia
[10] ROXIE website. [Online]. Available: https://espace.cern.ch/roxie
[11] T. Gortsas et αl., "An advanced ACA/BEM for solving 2D large-scale problems with multiconnected domains", CMES: Computer Modeling in Engineering & Sciences, 107(4), pp. 321-343, 2015.
[12] ANSYS website. [Online]. Available: https://www.ansys.com/
[13] A. Pampaloni et al., "Preliminary Design of the Nb3Sn cosθ Short Mod-el for the FCC", IEEE Transactions on Applied Superconductivity, Vol. 31, No.5, Art. No. 4900905, August 2021.